



Numerical Simulation of Water-Rich Fault Fracture Zone of Tunnel Considering Fluid Solid Coupling

Ran Xu *, Jianhe Li, Miao Wang

Changjiang Survey, Planning, Design and Research Co., Ltd., Wuhan 430010, China

*xuran@cjwsjy.com.cn

Abstract. During the construction of tunnels when crossing water-rich fault fracture zones, large-scale water inrushes often occur, thus making the study of the mechanical mechanisms behind water inrushes in fault fracture zones scientifically significant. Based on the actual construction conditions of tunnel projects, the fundamental principles of groundwater seepage, and the theory of elastoplastic mechanics, combined with the engineering case of water inrush in the Xiaopu Tunnel, a mathematical model for tunnels crossing water-rich fault fracture zones is established. With the aid of Comsol, the variation patterns of the stress field and seepage field in the surrounding rock during tunnel excavation towards the fault zone are simulated. The conclusions drawn are as follows: After the tunnel excavation enters the fault fracture zone, the pore water pressure dissipates significantly, leading to an expanded unloading range of the surrounding rock, intensified stress relaxation. The displacement of the surrounding rock around the tunnel increases sharply and abruptly, and the tunnel seepage velocity increases markedly.

Keywords: Tunnel Engineering; Fault Fracture Zone; Water Inrush; Fluid-Solid Coupling

1 Introduction

During tunnel excavation, water inrush and mud bursts are primarily triggered by two geological conditions: karst phenomena and water-rich structures, which encompass adverse geological formations such as faults and contact zones of intrusive rocks [1]. Currently, there is a wealth of research on karst water inrush, whereas studies on water inrush from fractured rock masses in fault zones are relatively scarce [2]. In recent years, fault zones have frequently induced geological disasters such as water inrush and mud bursts in tunnels and other underground projects [3].

The geological conditions of fault fracture zones are extremely complex, with factors such as fault structure, degree of fragmentation, and water abundance posing threats to the stability and safety of tunnels [4]. This complexity makes it difficult for traditional mechanical analysis and empirical methods to accurately predict the risk of water inrush during tunnel excavation. The application of numerical simulation in tunnel engineering construction provides a scientific basis for tunnel design, construc-

tion, and risk control [5]. It also facilitates in-depth analysis of the evolution of seepage-induced damage in the filling medium, which is of great significance for studying the mechanism of water and mud inrush [6]. In recent years, scholars have utilized numerical simulation to investigate the multi-field coupling mechanism among stress field, displacement field, and seepage field when tunnels cross fault fracture zones and experience water and mud inrush [7,8].

This study, incorporating the engineering case of water inrush in the Xiaopu Tunnel, establishes a mathematical model for tunnels crossing water-rich fault fracture zones. With the assistance of Comsol, it simulates the variation patterns of the stress field and seepage field in the surrounding rock during the process of tunnel excavation up to the fault zone. It provides certain assistance for the conceptual design of tunnel projects, thereby offering technical guidance for ensuring subsequent construction safety.

2 Seepage-Stress Coupling Model

The fluid-solid coupling mathematical model for water inrush during tunnel excavation primarily includes seepage model and solid mechanics model. In this study, the conceptual model for multi-field coupling of tunnel water inrush is shown in Figure 1.

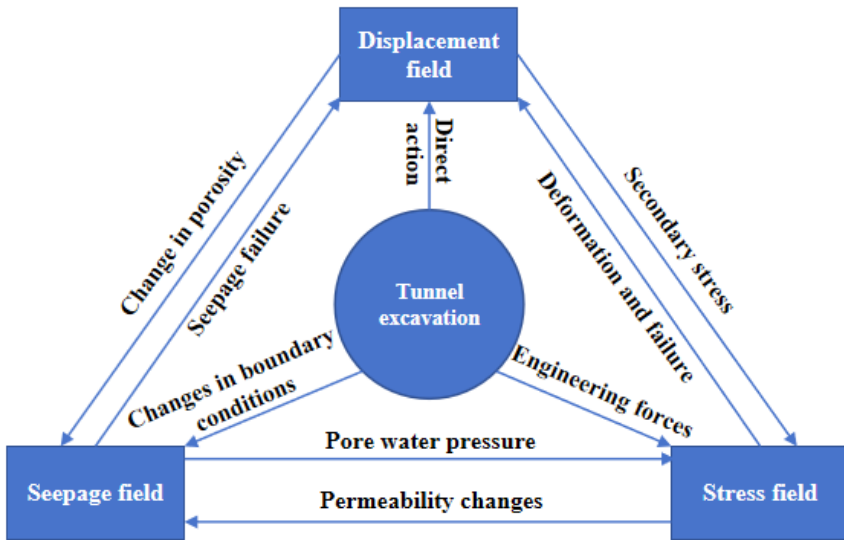


Fig. 1. Conceptual model for multi-field coupling of tunnel water inrush.

Numerical analysis of fluid-solid interaction is conducted using the Fluid Flow Module and Solid Mechanics Module in COMSOL, where the rock mass is treated as a homogeneous, isotropic equivalent continuous medium; the fluid is a single-phase, incompressible fluid, and its flow follows Darcy's law; deformation of the medium due to temperature changes is neglected, and the seepage field is considered to be in

an isothermal state; based on Terzaghi's principle of effective stress, the main coupling equations for the seepage field and stress field are as follows:

$$-\nabla \cdot \sigma = F_v, \quad \sigma = s \quad (1)$$

$$s - S_0 = C: (\varepsilon - \varepsilon_0 - \varepsilon_{inel}) + \left(\text{trace}(C: (\varepsilon - \varepsilon_0 - \varepsilon_{inel})/3 + p_w) \right) + \alpha_B p_f \quad (2)$$

$$\varepsilon = \frac{1}{2} [(\nabla u)^T + \nabla u] \quad (3)$$

$$\rho S \frac{\partial p_f}{\partial t} + \nabla \cdot (\rho u) = Q_m - \rho \alpha_B \frac{\partial e_{vol}}{\partial t} \quad (4)$$

$$u = -\frac{k}{\mu} (\nabla p_f + \rho g \nabla D) \quad (5)$$

$$S = \varepsilon_p \chi_f \quad (6)$$

In the equation: F_v represents the volumetric load (N/m^3); σ denotes the stress field; u represents the displacement field; p_w , p_f stand for pressure (Pa); α_B is the Biot-Willis coefficient; χ represents the compression ratio ($1/Pa$); μ represents the dynamic viscosity of the fluid ($Pa \cdot s$); and k is the permeability (m^2).

In this study, with reference to the research conducted by Ji et. al. [9], the relationship between geotechnical porosity, permeability coefficient, and effective stress is assumed to be:

$$\phi = \Phi_0 e^{-a\sigma}, \quad K = K_0 e^{-b\sigma} \quad (7)$$

In the equation: a and b are fitting constants, In this study, the value of a is $1.5e-7 Pa^{-1}$, and the value of b is $1.0e-7 Pa^{-1}$; Φ and K represent porosity and permeability coefficient, respectively; Φ_0 and K_0 represent the initial porosity and initial permeability coefficient, respectively.

3 Establishment of Tunnel Water Inrush Model

3.1 Project Overview

This study investigates the mechanism of water inrush in tunnels crossing fault zones, with a focus on the water inrush event at YX6+595.2 in the Xiaopu Tunnel of the Central Yunnan Water Diversion Project. The Xiaopu Tunnel is the starting point of the Yuxi section of the Water Diversion Project in Central Yunnan, with its entrance connecting to the Kunming section and equipped with a maintenance gate, and its exit connecting to the Adou Village Aqueduct. The tunnel crosses a total of four fault zones, including the Wangjiawan Fault and its secondary fault fracture zones (FVI-1, FVI-2, F32-1, F32-2), which are composed of cataclastic rocks, mylonites, fault breccias, and fault gouge, intersecting the tunnel at medium angles.

At 4:00 AM on May 1, 2021, when the upstream of Xiaopu Tunnel's No. 2 branch tunnel was excavated to YX6+595.2, sand inrush occurred at the right arch crown of the tunnel face. At this time, the tunnel was buried at a depth of 100~102.5 meters,

with a groundwater head of 100 meters, and the surrounding rock was composed of grayish-white and steel-gray thin-layered dolomite of the Sinian Dengying Formation (Zbdn). On the afternoon of May 13, at 4:40 PM, the mud inrush had flooded 200 meters of the tunnel (approximately 3,260 cubic meters of mud, as shown in Figure 2).



Fig. 2. Water Inrush at YX6+595.2 of Xiaopu Tunnel.

3.2 Numerical Model

The tunnel has an average burial depth of 100m and an average groundwater head height of 100m within the F32-2 fault zone; the tunnel has a diameter of 6m and a height of 13m. The fault is approximately 34m wide and has an inclination angle of 60° . Excavation of the underground cavern primarily affects the stress and displacement of the surrounding rock within a range of 3 to 5 times the tunnel diameter centered on the cavern. Beyond 3 times the tunnel diameter, the influence is less than 5%. Therefore, the horizontal dimensions of the computational model extend 60m from the tunnel axis on each side. Vertically, the lower boundary is set 50m below the tunnel's central axis, and the upper boundary reaches the static water level, which is 100m above the tunnel's central axis.

Additionally, when the tunnel face is constructed within a range of 0.75 to 1.25 times the tunnel diameter from the fault, significant changes occur in the stress and displacement of the surrounding rock. Thus, the longitudinal scope of the computational model should also be extended accordingly, by 58m on each side from the fault. The entire computational model has three-dimensional dimensions of 120m x 150m x 150m, as shown in Figure 3.

The main focus of this study is mechanism of water and mud inrushes in tunnels crossing fault zones. Therefore, the simulation of tunnel excavation construction has been appropriately simplified: The tunnel adopts full-section excavation, with an excavation step distance of 2m before entering the fault zone and changed to 1m when approaching the fault zone; the excavation distance in ordinary surrounding rock is 70m, and in the fault zone is 20m, totaling 90m of excavation.

For the convenience of calculation and modeling, the surrounding rock in the computational model is considered as two types: ordinary surrounding rock and fault

zone. The values of the calculation parameters are mainly referenced from Weng's research [10], as shown in Table 1.

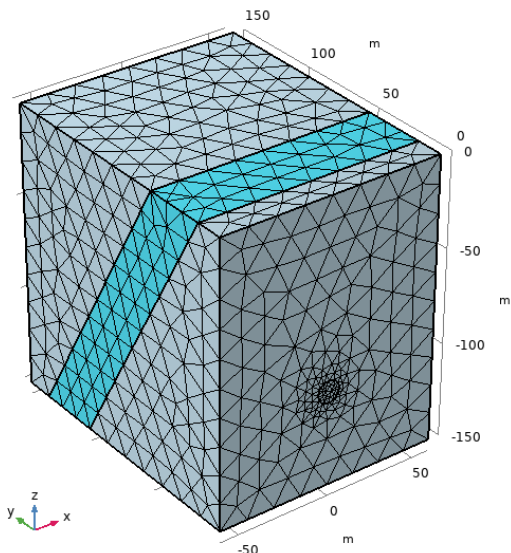


Fig. 3. Water Inrush at YX6+595.2 of Xiaopu Tunnel.

Table 1. Physical and Mechanical Parameter Values for Surrounding Rock.

Material	Elastic modulus (GPa)	Unit weight (kN/m ³)	Poisson's ratio	Friction angle (°)	Cohesion (MPa)	K ₀ Φ ₀ (cm/s)
Surrounding rock	2.93	20.4	0.30	25	0.8	0.29.8e-5
Fault zone	1.10	16.3	0.45	20	0.5	0.3 2.9e-4

4 Calculation Results and Analysis

4.1 Pore Water Pressure

During the tunnel excavation through the fault fracture zone, the variation in pore water pressure field of the surrounding rock is illustrated in Figure 4. Below are the cross-sectional views of pore water pressure distribution when the tunnel face is excavated to 0m, 30m, 76m, and 90m.

Before excavation, the initial pore water pressure in the tunnel's surrounding rock increases with depth, similarly in both ordinary rock and the fault zone. After excavation, significant changes occur, with lower water pressure forming a funnel-like zone around the tunnel. When entering the fault zone, pore water pressure drops significantly and expands further. From 30m to 90m excavation, the maximum pore water pressure decreases by 34.68%, from 1.24MPa to 0.81MPa.

The simulation results reveal that when the tunnel crosses the fault zone, the pore water pressure dissipates significantly, leading to an increase in hydraulic gradient, which in turn causes an increase in seepage velocity and osmotic dynamic water pressure. As a result, groundwater is more likely to infiltrate into the tunnel, thereby exacerbating the instability and failure of the rock mass in the faulted and fractured zone.

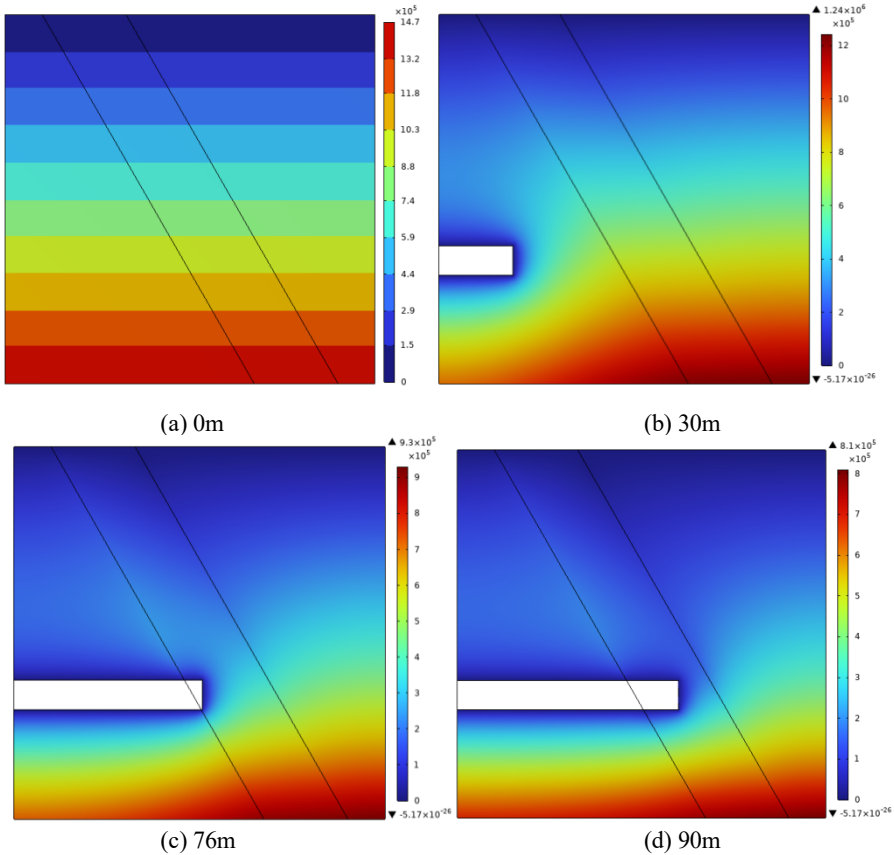


Fig. 4. Pore water pressure contour map of surrounding rock (Unit: Pa).

4.2 Stress

During the tunnel excavation process through the fault fracture zone, the variation in Mises stress of the surrounding rock is shown in Figure 5. A cross-section located 10m behind the tunnel face is taken as the monitoring section. Below are the contour plots of Mises stress distribution on the monitoring section when the tunnel face is excavated to 30m, 60m, 76m, and 90m.

Before entering the fault zone, as the tunnel excavation progresses, the maximum Mises stress in the surrounding rock gradually increases, and stress concentration intensifies. When the tunnel is excavated to 30m, the maximum Mises stress reaches

3.83 MPa. As the tunnel approaches the fault zone at 68m (excavation depth of 68m), stress concentration reaches its peak, with the maximum Mises stress reaching as high as 4.06 MPa. After the tunnel enters the fault zone (excavation depth of 90m), the Mises stress decreases to 2.56 MPa, and the stress distribution pattern transforms from a "butterfly-shaped" distribution before entering the fault zone to a similar "arch-shaped" distribution around the tunnel perimeter.

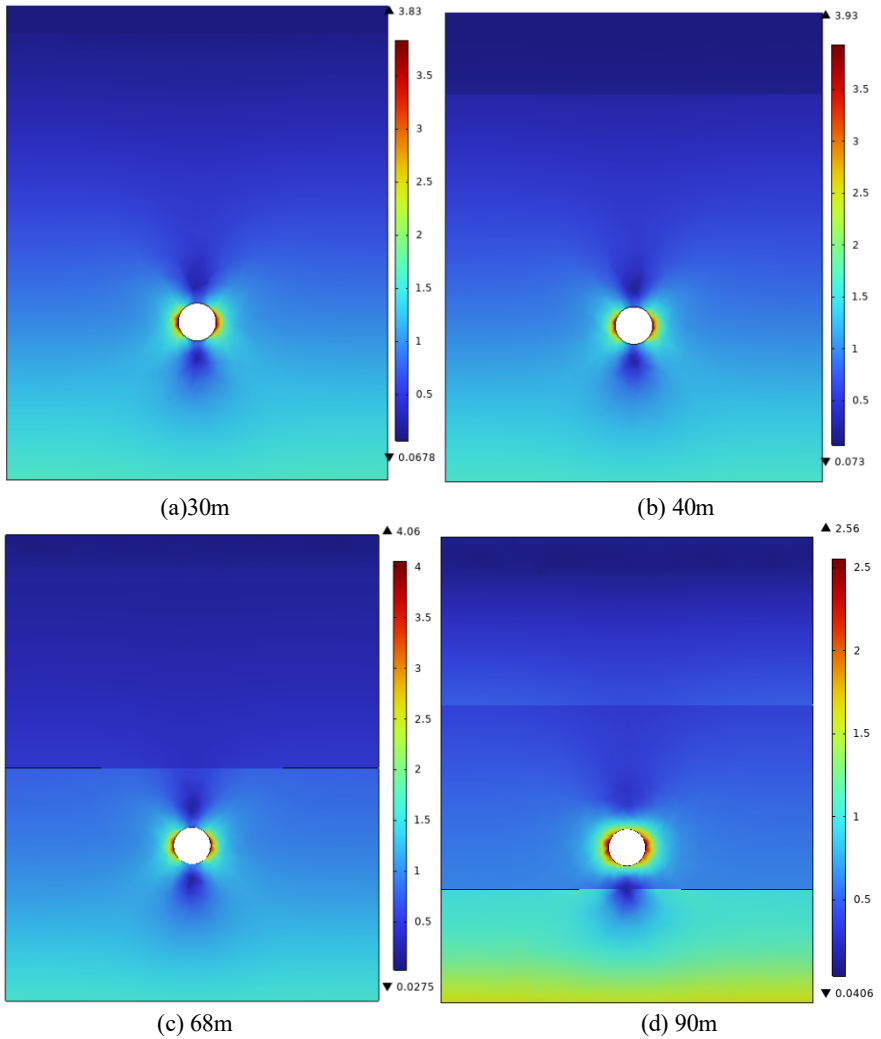


Fig. 5. Mises stress contour map of surrounding rock (Unit: MPa).

When tunnel traverses fault zone, a large-scale stress release occurs, causing the rock mass to release energy towards the excavation face of the tunnel through forms such as dilatancy failure. According to Equation (7), this will lead to the expansion

and development of pores in the surrounding rock of the tunnel, increasing its permeability and facilitating the occurrence of water inrush disasters.

4.3 Displacement

During the tunnel excavation through the fault fracture zone, the changes in the crown displacement, and lateral displacement of the surrounding rock are shown in Figure 6. Before the tunnel excavation reaches the fault, the displacement values remaining basically stable near a relatively small value. As the tunnel excavation progresses from 30m to 60m, the crown displacement changes from 4.61mm to 5.19mm, with an increase of only 12.58%. The lateral displacement undergoes even smaller changes, shifting slightly from 1.47mm to 1.48mm. As the tunnel excavation advances towards the fault, all displacement values exhibit sharp and abrupt increases. When the tunnel excavation reaches 90m, it has penetrated deeply into the fault zone, the crown displacement value reaches 11.5mm, an increase of 149.45% compared to when the excavation was at 30m.

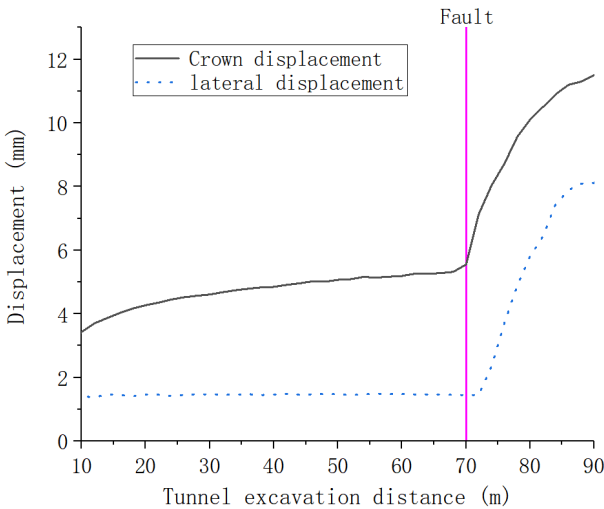


Fig. 6. Tunnel excavation distance-displacement curve.

4.4 Flow Velocity

After tunnel excavation, the distribution of the seepage velocity field is shown in Figure 7. Before the tunnel excavation enters the fault zone area, the groundwater flow is relatively stable with minor changes in velocity. When excavated to 50m, the maximum seepage velocity is 9.44×10^{-6} m/s. Upon entering the fault zone during tunnel excavation, the flow velocity undergoes abrupt changes, showing a sudden and sharp increase. When excavated to 90m, the maximum seepage velocity reaches 2.15×10^{-5} m/s, representing an increase of up to 127.75%.

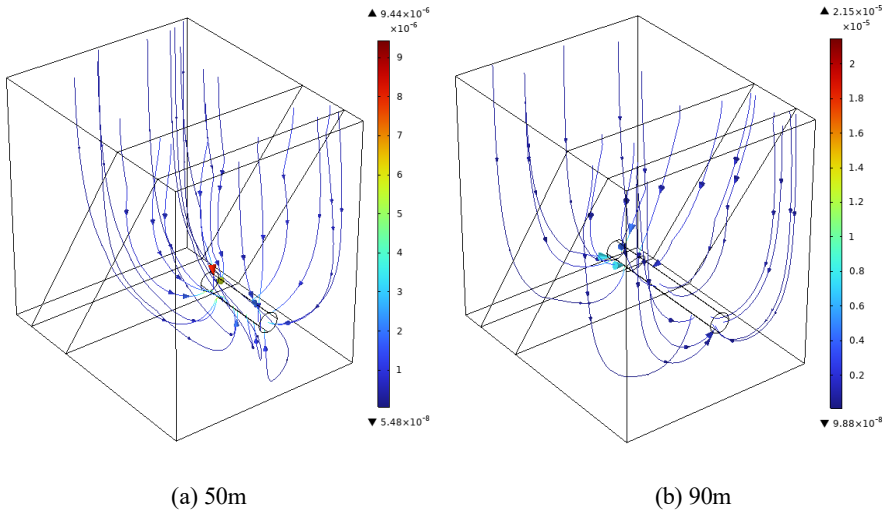


Fig. 7. Fluid streamline of seepage in surrounding rock.

5 Conclusions

This study, combining the engineering case of water inrush in the Xiaopu Tunnel, employs the COMSOL multiphysics coupling numerical simulation software to simulate and analyze the variation patterns of stress field, displacement field, and seepage field during the process of tunnel excavation into the fault zone. The conclusions drawn are as follows: After the tunnel excavation enters the fault fracture zone, the pore water pressure dissipates significantly, leading to an expanded unloading range of the surrounding rock, intensified stress relaxation. The displacement of the surrounding rock around the tunnel increases sharply and abruptly, and the tunnel seepage velocity increases markedly.

Acknowledgments

This research was funded by a fellowship from the Major Science and Technology Project of the Ministry of Water Resources (no. SKS-2022103), a fellowship from the China Postdoctoral Science Foundation (no.2024M762779), and a fellowship from the post-doctoral innovation practice positions in Hubei province (no. 2024HBBHCXB084), a fellowship from the Independent Innovation Project of Changjiang Design Group (CX2021Z01).

References

1. Xue, Y., Kong, F., Li, S., Qiu, D., Su, M., Li, Z., & Zhou, B. 2021. Water and mud inrush hazard in underground engineering: genesis, evolution and prevention. *Tunnelling and Underground Space Technology*, 114, 103987.
2. Wan, F., Xu, P., Zhang, P., Qu, H., Wang, L., & Zhang, X. 2021. Quantitative Inversion of Water-Inrush Incidents in Mountain Tunnel beneath a Karst Pit. *Advances in civil engineering*, 2021(1), 9971944.
3. Yang, W., Fang, Z., Wang, H., Li, L., Shi, S., Ding, R., ... & Wang, M. 2019. Analysis on water inrush process of tunnel with large buried depth and high water pressure. *Processes*, 7(3), 134.
4. Cao, Z., Gu, Q., Huang, Z., & Fu, J. 2022. Risk assessment of fault water inrush during deep mining. *International Journal of Mining Science and Technology*, 32(2), 423-434.
5. Cao, A., Wu, J., Chu, W., Wang, D., & Cheng, Y. 2023. Comparative study on tunnel boring machine and drilling-blasting methods for tunnels based on FLAC3D. In *Third International Conference on Mechanical Design and Simulation (MDS 2023)* (Vol. 12639, pp. 785-790). SPIE.
6. Hui, H., Bowen, Z., Yanyan, Z., Chunmei, Z., Yize, W., & Zeng, G. 2018. The mechanism and numerical simulation analysis of water bursting in filling karst tunnel. *Geotechnical and Geological Engineering*, 36(2), 1197-1205.
7. ZHOU, Z. Q., LI, L. P., SHI, S. S., LIU, C., GAO, C. L., TU, W. F., & WANG, M. X. 2021. Study on tunnel water inrush mechanism and simulation of seepage failure process. *Rock and Soil Mechanics*, 41(11), 6.
8. Yu, H., Zhu, S., & Hou, J. 2020. Numerical simulation of water inrush in fault zone considering seepage paths. *Natural Hazards*, 104, 1763-1779.
9. Ji Youjun, Liu Jianjun, Cheng Linsong. 2011. Numerical simulation of tunnel excavation considering fluid-solid coupling [J]. *Rock and Soil Mechanics*, 32(4): 1229-1231. (in chinese)
10. WENG Xianjie. 2014. Study on inrush of water and mud mechanism and grouting control technology in water-rich fault fracture zone of tunnel [D]. Jinan, Shandong University.

Open Access This chapter is licensed under the terms of the Creative Commons Attribution-NonCommercial 4.0 International License (<http://creativecommons.org/licenses/by-nc/4.0/>), which permits any noncommercial use, sharing, adaptation, distribution and reproduction in any medium or format, as long as you give appropriate credit to the original author(s) and the source, provide a link to the Creative Commons license and indicate if changes were made.

The images or other third party material in this chapter are included in the chapter's Creative Commons license, unless indicated otherwise in a credit line to the material. If material is not included in the chapter's Creative Commons license and your intended use is not permitted by statutory regulation or exceeds the permitted use, you will need to obtain permission directly from the copyright holder.

